

# The effect of tamper layer on the explosion dynamics of atom clusters

Zoltán Jurek\* and Gyula Faigel

*Research Institute for Solid State Physics and Optics*

*H 1525 Budapest, POB 49, Hungary*

(Dated: August 27, 2021)

## Abstract

The behavior of small samples in very short and intense hard x-ray pulses is studied by molecular dynamics type calculations. The main emphasis is put on the effect of various tamper layers about the sample. This is discussed from the point of view of structural imaging of single particles, including not only the distortion of the structure but also the background conditions. A detailed picture is given about the Coulomb explosion, with explanation of the tampering mechanism. It is shown that a thin water layer is efficient in slowing down the distortion of the atomic structure, but it gives a significant contribution to the background.

PACS numbers: 61.80.-x, 36.40.-c, 61.46.+w

Keywords: femtosecond, x-ray, cluster

---

\*Electronic address: jurek-z@szfki.hu

## I. INTRODUCTION

Today's most important tool for structure determination is x-ray crystallography. This method works only on samples having spatial periodicity. However, there is a growing need for the determination of the atomic order of small non-periodic entities such as biomolecules, individual nanoparticles, atomic clusters etc. Since in these systems the radiation damage is not distributed randomly among a huge number of identical units (elementary cells in crystals), the average structure significantly changes with any single damage event. Therefore the structure determination of these particles requires a different approach than that of crystalline substances. A solution, which avoids geometrical distortion was suggested by Solem et al. [1, 2] and later it was extended to biomolecules by Neutze et al. [3]. Their idea was catalyzed by the construction of future x-ray free-electron lasers (XFELs) [4, 5], which will provide extremely bright hard x-ray beam with very short pulses. According to their reasoning elastically scattered photons should be collected during the very short and intense pulse of XFELs. Although in long term the radiation damage is fatal (the sample explodes), in extremely short times, the atoms of the sample do not move appreciably. Limiting the collection of elastically scattered photons to this period we could obtain useful data for the original structure of the sample. The key question in this case is the dynamics of the sample explosion: How much time do we have for imaging? Various models have been worked out to describe the behavior of the sample in the beam [6, 7, 8]. Although the explosion dynamics predicted by these models slightly differ in details, but they all arrive at the same general conclusion: to do successful imaging with atomic resolution one needs shorter pulses than the pulse length of the presently constructed sources. Since the realization of shorter pulses is not simple, there is a search for methods by which the useful time interval for the measurement of elastically scattered photons could be extended. A suggestion to delay atomic motion was put forward by Hau-Riege et al. [8]. They would surround the particle by a tamper layer. In the case of biological molecules this layer would naturally be a water shell. However, the effect of this layer is not trivial. Lately, Hau-Riege et al. published model calculations, which examined this possibility [9]. They concluded that a tamper water layer delays the explosion of the inner part of the sample, and they suggested that pulses with width of 50 fs or even larger could be used for atomic resolution imaging of single bio-molecules. Their model calculations were based on a 1D continuum approach.

Since the parameter range used in their calculations is not available at the present technical level, it is very difficult to check the validity of the various simplifications. A more detailed and realistic picture could be given by molecular dynamics modeling. However, the CPU requirement of these calculations increase very fast with the number of particles, therefore it is difficult to model large enough systems. We have developed a special MD algorithm for the description of the dynamics of a small atom-cluster (or a molecule) in the intense x-ray pulse [6, 10]. Lately, we improved this code to a highly parallelized form. Using this program we are able to model systems with similar sizes as in Hau-Rieges paper. So we did a series of calculations, partly to check the conclusions of the simpler continuum approach, and partly to get a more detailed picture of the Coulomb explosion of atom-clusters.

The paper consist of 6 parts: after the introduction (part I) we give a brief general description of the explosion process, describe the main features of our model, and compare our results with that of Hau-Rieges (part II). In part III we discuss the effect of the composition of the tamper layer. In part IV we give an estimate for the unavoidable background contributions and discuss the effect of pulse length and shape. In part V we show the result of model calculations starting from the parameters satisfying the requirement given by the classification. At last in part VI our results are summarized and conclusions are drawn.

## II. COMPARISON OF THE EXPLOSION DYNAMICS OBTAINED FROM THE CONTINUUM AND MOLECULAR-DYNAMICS MODELS

In the proposed single molecule imaging experiments, individual identical molecules will be exposed to XFEL pulses one-by-one in random, unknown orientation. Estimates for the number of elastically scattered photons show that single diffraction patterns will be very noisy, due to photon counting statistics. So the compilation of a 3D diffraction pattern, which is necessary to solve the structure is not possible directly from the individual 2D images. One has to collect many pictures into each orientation bins, and add these to improve statistics. This means that the minimum requirement of photon counting statistics is determined by the ability to classify the diffraction patterns according to their orientation.

Model calculations of the classification process [11] give us a good estimate for the number of photons as a function of the required real space resolution. Based on the work of G. Bortel and G. Faigel [11] we are considering XFEL pulses with energy of 12 keV and with fluence

in the range of  $10^{13} - 10^{14}$  photons/pulse. As pulse length we use 10 and 50 fs, which is shorter than the pulse length of XFEL-s under construction but it is realistically reachable. The reason of using this very short pulse width is that even under this short time, atoms might move appreciable distances. The pulse shape might also influence the imaging of the atomic structure, therefore we consider flat top and Gaussian shapes.

After defining the beam parameters we briefly outline the processes governing the behavior of the sample under the influence of the x-ray pulse. Approximately  $10^{13}$  photons are focused to a 100 nm spot, in which our sample is situated. Three direct interactions are considered: Compton scattering, elastic scattering and photoionization. The first interaction is the smallest, and gives a negligible continuous background. Part of the elastically scattered photons carry the information on the structure, these are what we want to select and use later for the structure determination. The other part contributes to the background (see detailed description later). The dominant process is however the third, the photoionization. This process leads to damage. It produces electrons with energy close to the incident photon energy, and also with lower energy indirectly through the Auger process. The energy of these slow electrons depends on the elements and for C, N, O which are the main constituents of biological samples it lies between 250 – 500 eV. The appearance of these electrons is a few fs after excitation.

Both high and low energy electrons scatter elastically and inelastically on the atoms and ions of the sample. Since the elastic scattering does not deposit energy in the sample it does not contribute directly to the damage process. It only modifies the path of electrons, and through this, it may slightly change the number of inelastic events. Concerning damage, the inelastic scattering (often called impact ionization or secondary ionization) of electrons is the most important. The cross section of this process is large for low energy electrons. Therefore the contribution of Auger electrons is dominant in this respect. At later times when electrons slow down recombination processes also take place. However, these processes come into play in the developed phase of the Coulomb explosion, so they are not important from the point of view of imaging. All the above processes are taken into account in our molecular-dynamics type model. The detailed description of this model is given in [6].

Based on this model we arrived at the following picture of the Coulomb explosion [6]. The main driving force of the explosion is the K shell photoionization. Photoelectrons leave the system with  $\sim 1/7$  light speed leading to a positively charged particle. Following this

the hollow atoms relax through Auger decay, emitting electrons of a few hundred eV energy. If the system is not too large (less than hundred Angstrom), most of the Auger electrons also leave the system in the early time of the pulse. However, as the positive charge of the particle increases first Auger and later for large molecules even photoelectrons cannot escape. These non-bound electrons further ionize atoms by impact ionization resulting even more free electrons with lower and lower energy. Parallel with these processes, gradually a rearrangement of the originally homogeneous charge distribution takes place. An almost neutral inner core and a highly positively charged outer shell develop. In the inner part, the free electron cloud screens the Coulomb force between the positive ions. In an earlier work [6] we have shown that the velocity of the particles in the inner core is much slower than in the outer shell. As a result the explosion of the core is slower than the explosion of the shell. This picture naturally leads to the application of sacrificial tamper layer, suggested by Hau-Riege et al [8]. The question is that what type of layer is the best, and within which conditions.

First, we compare our results with that of Hau-Rieges [9]. In [9] the authors found that about 10 Å thick water tamper layer is optimum for imaging, since it effectively slows down the explosion of the inner part and at the same time it gives the smallest contribution to the elastic x-ray background. Therefore we performed a calculation for an 80 Å diameter particle, composed of a 30 Å radius core (the sample) containing C atoms and a 10 Å thick water tamper layer. A 10 fs flat top x-ray pulse hit the sample. The pulse contained  $10^{13}$  12 keV photons focused to a 100 nm spot. In Fig. 1 the relative displacement of the atomic shells are shown as a function of time for each element (H (a), O (b), C (c)) independently.

As a reference we also plotted on this figure the displacement of C atoms (d) for a 30 Å radius cluster without the water tamper layer. It is clear that the explosion of the sample is milder applying the tamper layer. So our conclusion agrees with that of Hau-Rieges. Looking at the numbers, we find that at the end of the pulse the outer layer of the sample moves about 3 Å in the case of no tamper layer and 1 Å with tamper layer. Beside the sample itself it is interesting to analyze the motion of the tamper layer. There are characteristic differences between Hydrogen and Oxygen atoms: first hydrogen moves faster and correspondingly larger distances, secondly H atomic shells are intermixed with oxygen. The first observation is trivial since one expects that lighter atoms move faster, because the  $q/m$  ratio ( $q$  is the ionization level of the atom, and  $m$  is the mass of the nucleus) is higher for

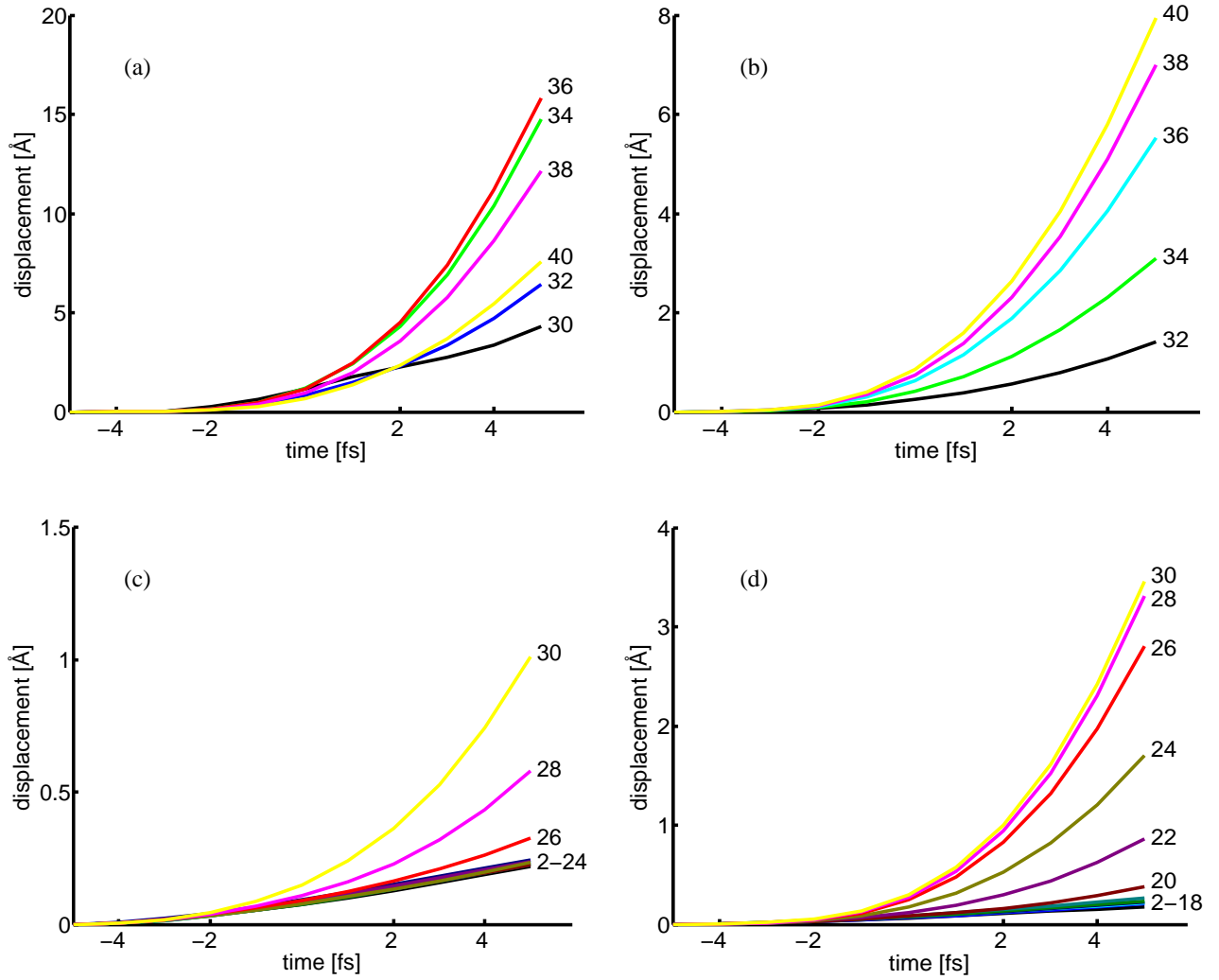


FIG. 1: (Color online) Relative displacement of the atomic shells as a function of time for H (a), O (b), C (c) during the Coulomb explosion of a small particle composed of a 60 Å diameter sample surrounded by 10 Å water. The time scale is chosen in such a way that zero time corresponds to the center of the pulse (half pulse). As a reference the displacement of C atoms (d) for a 60 Å diameter cluster without the water tamper layer is also plotted.

H. However, the second feature is surprising: H atoms originally located at the central part of the water shell move faster than atomic shells at larger distances (Fig. 1.a). This feature can be explained by the different ionization mechanism of Hydrogen as compared to Oxygen and Carbon atoms. The photoionization of Hydrogen is negligible relative to the impact ionization. Therefore slow electrons generated by the Auger process on Oxygen and Carbon (and consecutive impact ionizations) ionize more effectively the Hydrogen. However, the

effect of these electrons is the highest in the central part of the water layer. The reason for this is threefold: i. Oxygen photoionization cross section is higher than that of Carbon; ii. Hydrogen atoms are close to Oxygen; and consequently Oxygen atoms produce more Auger electrons in a shorter time than Carbon. iii. A large part of Auger electrons produced at the outer edge of the water shell leave the system without interaction (going radially out). All these lead to a faster ionization of Hydrogen atoms being in the central part of the water shell and consequently larger coulomb forces and faster explosion.

At the end of this section we show three more characteristics of the explosion, which naturally comes out from our model, but they are difficult to derive from the continuum approach. The first is the real space image of the atomic arrangements at different times (Fig. 2). We chose three times: the zero time (a) (at the beginning of the pulse, the original particle surrounded by the water shell), at half time (b) (when half of the photons in a pulse hit the sample) and at the end of the pulse (c).

We show two sets of images: the original sample without tamper layer (a, b, c) and the sample with the tamper layer (d, e, f). Looking at these images one can get a clearer picture of the explosion in real space. In the upper part of the figure the bare sample is shown. The development of a thin distorted layer is clearly visible. This points to the application of sacrificial tamper layer. In the lower part of Fig. 2, the sample surrounded by a 10 Å thick water layer is shown. It is clear from the lower right panel that in this case the original atomic arrangement of the sample does not change significantly during the pulse. From this figure it is also clear, that the background coming from the water shell will be a composite picture; an average of the changing positions of Oxygen and Hydrogen atoms (ions). The second characteristic is the spatial distribution of electrons (Fig. 3).

The 3D arrangement of electrons (yellow spheres) is shown at the end of the pulse. In Fig. 3.a a large scale view, while on Fig. 3.b a zoomed image of the electrons are shown. On the large scale a butterfly shape form composed of photoelectrons and in the center, at the place of the sample, a small nucleus built up from Auger and secondary electrons can be seen. The anisotropic distribution of photoelectrons is a result of the linearly polarized incident beam. At this scale one cannot distinguish individual electrons at the center. However, on the zoomed scale in Fig. 3.b - in contrast to the photoelectron distribution -, an almost isotropic arrangement of Auger and secondary electrons is clearly shown. Beside the spatial distribution of electrons, it is very useful to plot the net local charge as a function of the

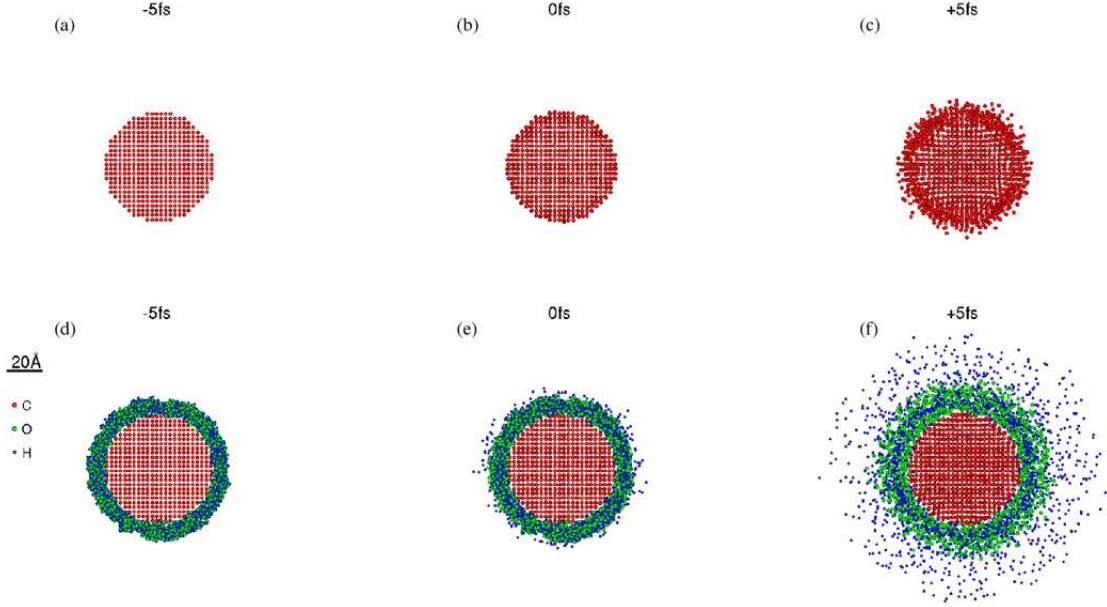


FIG. 2: (Color online) Real space image of the atomic arrangements at different times during the x-ray pulse for the same pulse and particles as in fig. 1. The atoms and ions are only shown in the cross section through the center of the sample. Upper panel: sample without tamper layer at the beginning of the pulse, at half time and at the end of the pulse (a, b, c), respectively. Lower panel: sample with tamper layer at the beginning of the pulse, at half time and at the end of the pulse (d, e, f), respectively.

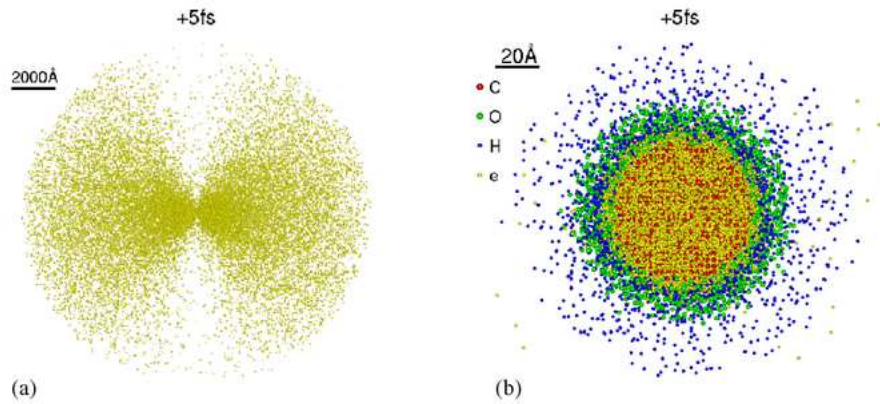


FIG. 3: (Color online) The spatial distribution of electrons for the same particle and pulse parameters as in fig. 1. The sample with the tamper layer is shown only. The arrangement of electrons is shown at the end of the pulse in large scale view (a) and in a smaller scale (b).



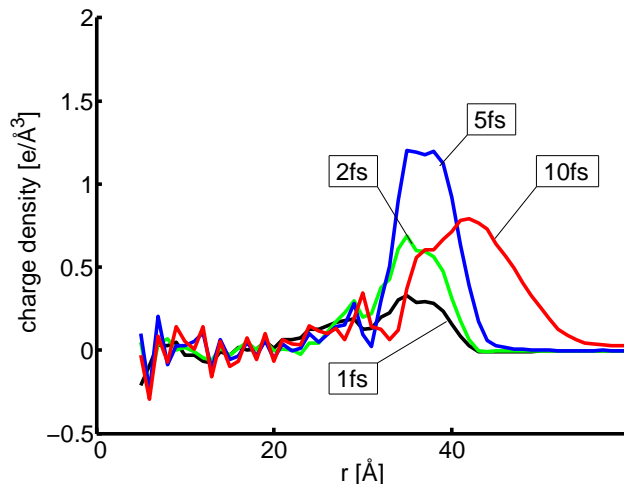


FIG. 4: (Color online) Net local charge as a function of the radial distance from the center of the sample at different times (1, 2, 5, 10 fs).

radial distance from the center of the sample. This is shown in Fig. 4 at different times during the pulse.

In a relatively short time from the beginning of the pulse between 1–2 fs an almost neutral core surrounded by a positively charged shell develops. This explains why the explosion of the sample is delayed by the use of tamper layer. This type of behavior has been predicted by our earlier calculations for smaller particles [6]. However, in those calculations there was no tamper layer, so the outer part of the sample was blown out fast. The replacement of this outer part by a sacrificial tamper layer is a natural, good idea. However, the composition of this layer is not trivial.

### III. THE CHOICE OF TAMPER LAYER

In this section we examine the effect of the composition of the tamper layer on the explosion dynamics. The tamper layer basically acts in two ways: i. it produces electrons, which might diffuse into the central part (into the sample itself), and ii. the nuclei of the tamper layer are a barrier for the atoms of the inner part, these cannot cross this layer easily.

The first effect leads to two things: a.) these excess electrons can cause secondary ionization of the atoms in the sample. If this ionization is more effective than the ionization caused by the electrons produced in the sample part itself the tamper layer might even

speed up the Coulomb explosion, b.) the excess electrons can also increase the number of free electrons in the central part. These electrons rearrange so that they help to form the neutral core ie. they facilitate the screening of the positive charges in the sample. Depending on the speed of the screening, this effect may slow down the explosion of the inner part. The balance of these two processes combined with the barrier effect of the nuclei of the tamper layer determines the dynamics of the Coulomb explosion. Since both the barrier effect and the electron production depend on the atomic number, we carried out model calculations for tamper layers composed of elements with different atomic number. We chose Helium, Carbon, Nitrogen, Oxygen, Argon and water. The water does not fit into the line since it is a two component system. We included it because it is the most natural cover layer for bio-molecules. Calculations were done for 20 Å radius samples, covered by layers with thicknesses chosen so that the total number of electrons in the layers was approximately the same as we find in a 10 Å thick water layer. The 20 Å radius was chosen as a compromise between CPU time and sample size. However, we emphasize here, that our calculations can be safely extrapolated for larger samples. To make this statement more evident, we show the results of a series of calculations for different sample sizes (6, 8, 10, 15, and 20 Å radiuses) covered by 10 Å water each. In Fig. 5 (red curve) the maximum displacements of the outer layer of the samples are shown as a function of sample size at the end of the pulse.

In all cases it remains below 1 Å indicating that the motion of the atoms themselves does not prevent the solution of the structure by this precision. However, there is an increase of the displacement with the size. Extrapolating this to larger distances would lead to too large atomic displacement for large samples. However, slightly increasing the thickness of the water layer (to 14 Å), and plotting the size dependence in this case (Fig. 5 green curve), we see that the increase of the displacement becomes much milder, (almost independent of the sample size). The conclusion is that the optimum layer thickness of water has to be scaled with the sample size. However, for smaller samples we should use the smallest thickness down to 10 Å in order to decrease the elastic x-ray background, without sacrificing resolution. Turning back to the original problem of tamper layer composition, we plotted the largest deviation of the samples outer layer for various tamper materials in Fig. 6.

There is a minimum at the C, at the samples own element. The light He does not help much because there is negligible photoionization of He, therefore no excess electrons help the screening of positive charges of the sample. Further the mass of He atoms is small,

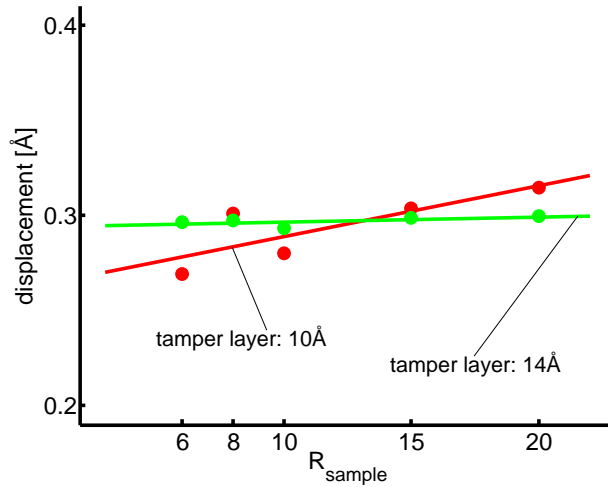


FIG. 5: (Color online) Maximum displacements of the outer layer of the samples as a function of sample size at the end of the pulse for 40 Å diameter samples covered by 10 Å (red curve) and 14 Å (green curve) water tamper layer.

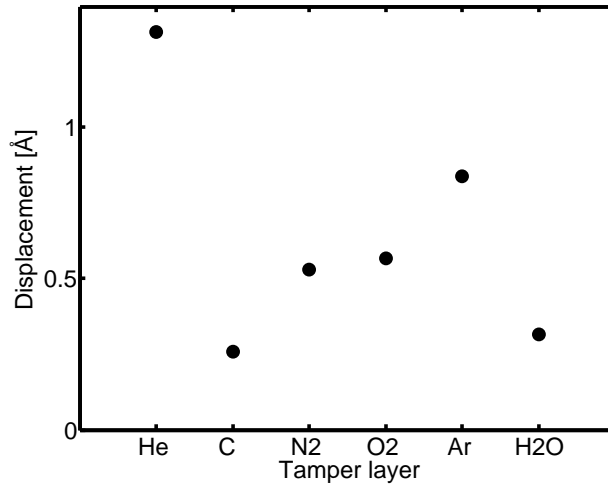


FIG. 6: The largest deviation of the sample's outer layer for various tamper materials.

they cannot significantly withhold C atoms from moving. On the other end of the line at the Argon the photoionization is significant but together with this there is a very strong secondary ionization of C atoms caused by the Ar's Auger and secondary electrons. This speeds up the explosion of the sample outer layers, and this is not compensated by the larger mass of Ar atoms, because the atomic density of Ar is very low, so they cannot withhold the Carbon atoms. The effect of the water layer is close to that of the pure carbon. The reason

is that the Auger electrons of O are very effective in the secondary ionization of Hydrogen, therefore many excess electrons are traveling into the Carbon sample. Even though these ionize the Carbon atoms by secondary ionization, the mass of the Oxygen atoms combined with the large atomic density of oxygen compensate for this and slow down effectively the explosion.

#### IV. THE EFFECT OF PULSE PARAMETERS AND TAMPER LAYER ON THE BACKGROUND

In previous sections we analyzed the x-ray pulse induced motion of the atoms. However, this is not the only problem of imaging. 2D diffraction patterns taken during consecutive pulses have to contain enough information for successful classification, ie. for finding patterns of particles arriving into the beam with the same orientation. This step is crucial, since without it the assembly of 3D diffraction pattern fails, and consequently the structure solution is not possible. The success of classification is strongly background dependent. Therefore in this section we give an estimate of the background of an ideal measurement. The sources of unavoidable background are: elastically scattered photons by the free electrons, elastic scattering from the atoms ions of the tamper layer, elastic scattering of those atoms ions of the sample which moved more then the tolerance (the required resolution). The first two factors starts with the pulse and is integrated over the pulse duration following the time evolution of the number of free electrons and the changing scattering power of the ions of the tamper layer. The third factor is different; it gives some contribution only close to the end of the pulse. It adds a relatively small value to the background but at the same time it decreases the signal with the same amount. This contribution depends on the duration and shape of the pulse. We calculate these contributions for 10 and 50 fs flat top and Gaussian shape pulses. As a model system we take a 20 Å radius carbon sample surrounded by a 10 Å thick water layer. In Fig. 7 (a, b, c, d) we plot all three contributions as a function of the integrated number of incident photons for flat top and Gaussian shape pulses with 10 and 50 fs widths.

For comparison we also plotted the useful signal, the elastic scattering from the sample. It is clear that the largest part of the background is coming from the tamper layer. The second largest is the free electron contribution and the smallest part is coming from the

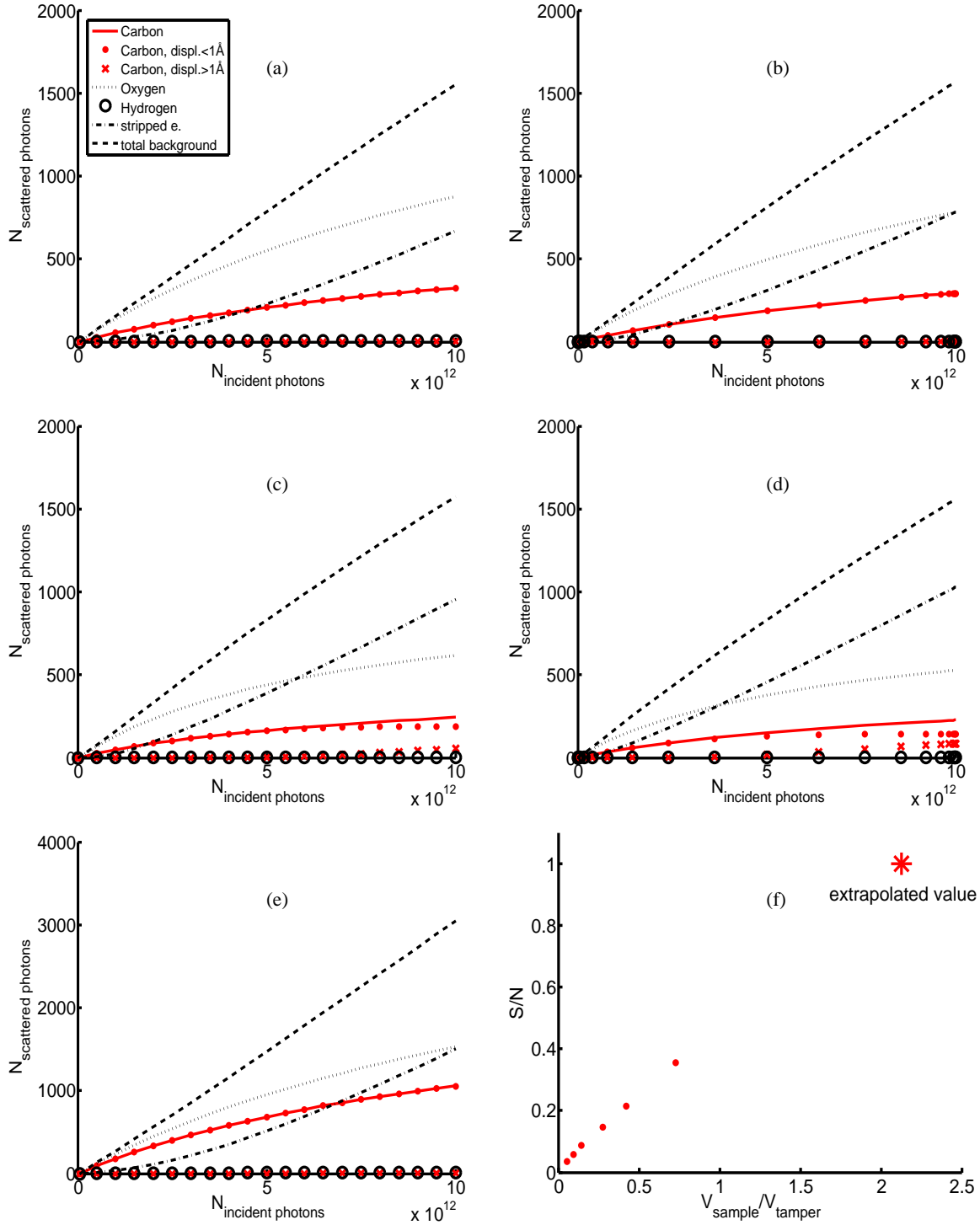


FIG. 7: (Color online) Background contributions and the useful signal of a 20 Å radius carbon sample surrounded by a 10 Å thick water layer as a function of the integrated number of incident photons for flat top (a, c) and Gaussian (b, d) shape pulses with 10 (a, b) and 50 (c, d) fs widths. Part (e) shows the same contributions as the previous parts for a 30 Å radius sample covered by 10 Å water in a flat top 10 fs wide pulse. In Part (f) the signal to noise ratio as a function of the sample volume normalized with the tamper layer volume is depicted. An extrapolated value is marked by a star.

deteriorating part of the sample. The total background is about three times larger than the signal. We can get a more promising picture by taking larger samples maintaining the same thickness for the tamper layer. In this case, the relative contribution of the tamper layer decreases. For illustration we show the background contributions for a 30 Å sample with 10 Å water (Fig. 7.e). It is very instructive to plot the signal to noise ratio as a function of the sample volume normalized with the tamper layer volume (Fig. 7.f). For 10 fs flat top pulses we obtain a linear dependence, and can safely extrapolate to larger sample sizes. We get S/N 1 for  $\sim 70$  Å radius samples. Further increase of the sample size results in an improved signal to noise ratio. However, for longer pulses (Fig. 7 c, d) -especially for the Gaussian shape-, the linear extrapolation does not hold. The reason for this is that in this case the background from the deteriorating part of the sample gets appreciable and at the same time the useful signal decreases significantly, lowering the signal to noise ratio. For a 50 fs Gaussian pulse the signal to noise ratio drops to about 0.06 for a 40 Å diameter sample covered by 10 Å water. This might cause significant problems in the classification and reconstruction process.

## V. MODELING BASED ON CLASSIFICATION REQUIREMENTS

So far we concentrated on the dynamics of explosion without analyzing whether the number of useful elastically scattered photons were enough to obtain any meaningful information on the structure. In this section we take into account the requirements given by the first step of data analyses the classification. Numerical modeling shows, that these requirements are the strictest among the steps of structure solution so the classification is the bottle neck in the evaluation process. Lately, G. Bortel and G. Faigel estimated the minimum number of photons necessary for classifications at various sample sizes [11]. Based on their results we did a series of calculations with more realistic input parameters. Classification considerations indicated the need of higher fluence on the sample. This can be reached either by using tighter focusing or by higher input intensity. We choose the second option and used  $10^{14}$  photons in a pulse with flat top shape leaving the focal spot 100 nm. The sample had 40 Å diameter surrounded by a 10 Å water shell. The time evolution of atomic shells is shown on Fig. 8.a.

The deterioration of the sample is drastic. The displacement of the outer shell is about

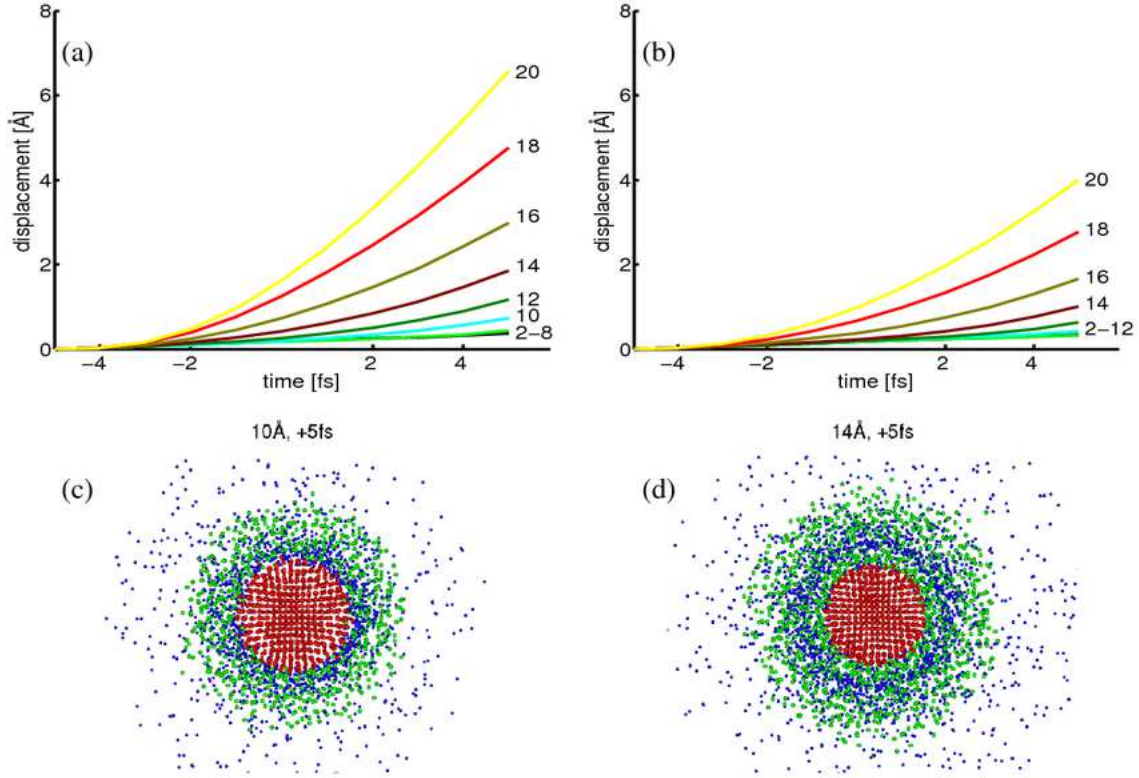


FIG. 8: (Color online) The time evolution of atomic shells of a 40 Å diameter sample surrounded by a 10 Å (a) and 14 Å (b) water shell for high fluence. The corresponding real space images at the end of the pulse are shown on parts (c) and (d), respectively.

8 Å at the end of the pulse. So imaging with atomic resolution is not possible. However, in section III we have seen that a small increase of the thickness of the tamper layer decreases the explosion of the core. Therefore we repeated the calculation for 14 Å water tamper layer. The displacement of the atomic shells is shown in Fig. 8.b. There is significant improvement; the largest deviation decreased two half compared to the 10 Å thick tamper layer. However even in this case we will have a degraded resolution. For illustration of the distortion we can expect we show the real space image of the atomic structure for the two tamper layers in Fig. 8.c and d. Further, we should also keep in mind that the price we pay for the reduced distortion is a tripled background caused by the larger amount of water.

## VI. SUMMARY AND CONCLUSION

We have examined the effect of tamper layers on the dynamics of Coulomb explosion of small Carbon particles in the XFEL beam. We found that a 10-14 Å water layer decrease the deterioration of the sample by a factor of three. The optimum thickness depends on the sample size and incident intensity. One should use thicker layer for larger size and for higher intensity. We also did a series of calculations for sacrificial layers composed of various elements (He, C, N, O, Ar). We found that very light (like He) and heavy (like Ar) elements are not effective in slowing down the Coulomb explosion of the sample. However, carbon, nitrogen and oxygen help in retaining the original atomic arrangement of the samples. The best result is shown by carbon. The effect of water layer is similar to the pure carbon case. Beside the explosion dynamics we also studied the various background contributions to the diffraction pattern of the sample. This is crucial from the point of the view of imaging the atomic structure. We found that the largest contribution is coming from the tamper layer. However, the weight of this contribution is decreasing for larger samples. We found that in the case of 10 fs flat top pulses the background is smaller than the signal, for samples larger than 70 Å in radius. However, for longer pulses the situation gets less favorable. For example the signal to noise ratio decreases to  $\sim 0.06$  for a 40 Å diameter sample illuminated by a 50 fs Gaussian pulse. This might be crucial concerning the possibility of single molecule imaging, since the first step of structure solution -the classification-, depends on the achievable statistics (SN ratio) reachable by a single shot.

Based on the requirements of the classification process we also modeled the Coulomb explosion at higher photon/pulse value (at  $10^{14}$  ph/pulse) than the design parameters of XFEL-s under construction. We found that the maximum displacement of atoms increases to about 8 Å (with 10 Å water layer) but it can be pushed down to 4 Å by increasing the thickness of the tamper layer. This may allow close to atomic resolution imaging. However, we pay for this with a significantly increased background i.e. a decreased SN ratio. Therefore further detailed numerical studies on the classification has to be done and probably new less noise sensitive classification methods has to be worked out. Our calculations indicate that in future experiments one has to do detailed preliminary modeling of the full imaging process in order to find the optimum experimental conditions for a given sample.



## Acknowledgments

The work reported here was supported by OTKA 67866 and NKFP1/0007/2005 grants. We thank Gabor Bortel and Miklós Tegze for the illuminating discussions.

---

- [1] J. C. Solem and G. C. Baldwin, *Science* **218**, 229 (1982).
- [2] J. C. Solem and G. F. Chapline, *Opt. Eng.* **23**, 193 (1984).
- [3] R. Neutze, W. Wouts, D. van der Spoel, E. Weckert, and J. Hajdu, *Nature* **406**, 752 (2000).
- [4] J. Arthur, *Linac coherent light source (lcls) design study report no. slac-r-521* (1998), [http://www-ssrl.slac.stanford.edu/lcls/design\\_report/e-toc.html](http://www-ssrl.slac.stanford.edu/lcls/design_report/e-toc.html).
- [5] F. Richard, J. R. Schneider, D. Trines, and A. Wagner, *Tesla technical design report no. 2001-11* (2001), [http://tesla.desy.de/new\\_pages/TDR\\_CD/start.html](http://tesla.desy.de/new_pages/TDR_CD/start.html).
- [6] Z. Jurek, G. Faigel, and M. Tegze, *Eur. Phys. J. D.* **29**, 217 (2004).
- [7] M. Bergh, N. Timneanu, and D. van der Spoel, *Phys. Rev. E* **70**, 051904 (2004).
- [8] S. Hau-Riege, R. London, and A. Szoke, *Phys. Rev. E* **69**, 051906 (2004).
- [9] S. P. Hau-Riege, R. A. London, H. N. Chapman, and A. Szoke, *Phys. Rev. Lett.* **98**, 198302 (2007).
- [10] G. Faigel, Z. Jurek, G. Oszlanyi, and M. Tegze, *Journal of alloys and compounds* **401**, 86 (2005).
- [11] G. Bortel and G. Faigel, *Journal of Structural Biology* **158**, 10 (2007).